

Publication V

Ari T. Alastalo, Markku P. V. Stenberg, and Martti M. Salomaa, *Response functions of an artificial Anderson atom in the atomic limit*, J. Low Temp. Phys. **134**, 897 (2004).

© 2004 by authors and © 2004 Springer Science+Business Media

Preprinted with kind permission from Springer Science+Business Media.

The original publication is available at www.springerlink.com.

<http://www.springerlink.com/openurl.asp?genre=article&id=doi:10.1023/B:JOLT.0000013208.27930.57>

Response functions of an artificial Anderson atom in the atomic limit

Ari T. Alastalo*, Markku P. V. Stenberg, and Martti M. Salomaa

*Materials Physics Laboratory, Helsinki University of Technology,
P.O.Box 2200 (Technical Physics), FIN-02015 HUT, Finland*

We consider the spin and pseudospin (charge) response functions of the exactly soluble Anderson atom model. We demonstrate, in particular, that a deviation from the magnetic Curie-law behaviour, appropriate for a free spin one-half, increases with increasing asymmetry and temperature. In general, oscillator strength is transferred from the spin degrees of freedom to the pseudospin modes. We also consider the negative- U Anderson atom and demonstrate that the pseudospin modes are the relevant low-energy excitations in this case. Especially, the roles of the spin and charge excitations are interchanged upon reversal of the intrasite Coulomb repulsion, U .

PACS numbers: 71.10.-w, 71.27.+a, 73.21.La, 75.75.+a

1. INTRODUCTION

A single quantum dot behaves like an artificial atom when electronic confinement in the dot approaches atomic size.¹⁻³ In such structures, there emerge the characteristic features of an atomic impurity: the quantization of charge and energy. It is appropriate to describe these artificial atoms by means of the Anderson impurity model.^{4,5}

The Anderson model was first proposed to describe magnetic impurities in a metal.⁶ In the Anderson model, the nonmagnetic-magnetic transition of the local d -state was first described within the Hartree-Fock (HF) approximation,⁶ which amounts to truncating the model Hamiltonian into

*Present address: VTT Information Technology, Tekniikantie 17, Espoo, FIN-02044 VTT, Finland; email: ari.alastalo@vtt.fi

Ari T. Alastalo, Markku P. V. Stenberg, and Martti M. Salomaa

a bilinear form in the fermion operators. This approximation leads to an abrupt phase transition, whereas the actual change must be a gradual one for a finite system. Numerous ingenious approaches to describe the complicated many-body problem associated with the emergence of the interacting correlated many-electron problem have been introduced, such as Green's function methods,⁷ functional-integral techniques,⁸ numerical renormalization schemes,^{9,10} Bethe-Ansatz approaches¹¹ and noncrossing approximations.¹² Perturbation theories have been utilized starting both from the small- U (HF) limit¹³⁻¹⁶ and from the atomic ($V_k = 0$) limit.^{17,18} Furthermore, interpolation schemes between the HF and atomic limits have been developed.¹⁹⁻²¹ However, the properties of the atomic limit, which again is exactly soluble, appears not to have been thoroughly discussed in the literature.²²

In this paper we want to discuss in detail the coupling of the correlations which takes place in the magnetic (zero-temperature susceptibility is divergent) Anderson atom. Relevant information on the correlations among the electrons may be obtained by considering the response of a system to an external perturbation. We derive the static response functions of the Anderson atom. Our derivation demonstrates that it is in general important to discuss not only the spin susceptibilities (χ) but also the charge (pseudospin²³) susceptibilities (ξ); the superscript zero in χ^0 and ξ^0 denotes static response.

We show that the Anderson impurity atom best follows the magnetic Curie law $\chi^0 = (4T)^{-1}$, appropriate for a quantum-mechanical spin one-half, in the symmetric situation at low temperatures ($T \ll U$). At high temperatures, on the other hand, the spin and charge degrees of freedom become equally important and the respective susceptibilities approach the common limiting value $T\xi^0 = T\chi^0 \rightarrow 1/8$ for $T \rightarrow \infty$ in zero field.

In particular, our equations may be applied to negative- U situations. The negative- U Anderson model was first proposed to describe the electronic structure of amorphous semiconductors.²⁵ Since then, negative- U behaviour has been observed, e.g., in the context of high-temperature superconductors,²⁶ heavy-fermion systems²⁷ and interstitial defects in semiconductors.^{28,29} It has been observed that in a quantum dot, the second electron in the dot may be more strongly bound than the first one under certain circumstances.³⁰⁻³⁴ Essentially two different mechanisms have been proposed to supply the effective net attraction between the electrons to cause a quantum dot negative- U properties.^{35,36} However, the microscopic origin of the phenomena is still unclear.

The reversal of U changes the roles of spin and charge. For the symmetric level configuration and negative U , the charge response functions behave like the spin susceptibilities for positive U . Hence, for $U \leq 0$, the spin degrees of freedom are frozen out and the charge degrees of freedom are the

Response functions of an artificial Anderson atom in the atomic limit

dominating low-energy excitations. In what follows, we intend to elucidate the dual roles played by the magnetic field in connection of spin dynamics and that of asymmetry in the context of charge dynamics.

For high magnetic fields, we find new peak structures in the longitudinal spin and charge susceptibilities and an associated threshold behaviour in the corresponding transversal response functions. These features are associated with level crossings occurring between states belonging to different Fock spaces in special configurations displaying high symmetry.

The rest of this paper is organized as follows. The Anderson Hamiltonian is presented in Section 2. In Section 3, we take a close look into the spin and charge algebras. Section 4 is devoted to derivation of analytic expressions for the spin and charge susceptibilities. In Section 5, we present our numerical results. In Section 6 we give discussion and conclusions. In Appendix A we collect the central properties of double-time Green's functions that are utilized throughout the present paper.

2. MODEL HAMILTONIAN

The Anderson Hamiltonian for magnetic impurities in metals⁶

$$\begin{aligned} \mathcal{H} = & \sum_{k,\sigma} \varepsilon_{k\sigma} n_{k\sigma} + \sum_{k,\sigma} \left(V_k c_{k\sigma}^\dagger d_\sigma + V_k^* d_\sigma^\dagger c_{k\sigma} \right) + \sum_{\sigma} E_{\sigma} n_{\sigma} \\ & + U n_{\uparrow} n_{\downarrow} \end{aligned} \quad (1)$$

describes the transition of the local d -electron orbital from a nonmagnetic resonant virtual bound state ($\Gamma/U \gg 1$) to a magnetic atom ($\Gamma/U \ll 1$). Here U is the intra-atomic Coulomb repulsion energy and $\Gamma = \pi N(0) \langle |V_k|^2 \rangle$ (with $N(0)$ the density of conduction electron states at the Fermi level, V_k the d -level hybridization matrix element and with $\langle \rangle$ denoting an average over the Fermi surface) is a measure of the admixture of the local state with energy $E_{\sigma} = E - \sigma B$ (here $\sigma = \pm 1/2$ and B is the external magnetic field). Furthermore, $c_{k\sigma}^\dagger$, $c_{k\sigma}$, d_{σ}^\dagger and d_{σ} are the creation and annihilation operators for electrons in the conduction band and in the impurity state, respectively, and the corresponding occupation-number operators are $n_{k\sigma} = c_{k\sigma}^\dagger c_{k\sigma}$ and $n_{\sigma} = d_{\sigma}^\dagger d_{\sigma}$. The conduction-electron dispersion relation is denoted with $\varepsilon_{k\sigma}$. In the nonmagnetic (d -spin susceptibility is finite at $T = 0$) $U = 0$ limit, the Hamiltonian (1) is of bilinear form and hence the static and dynamic properties of the impurity spin may be obtained exactly in closed form.³⁷ In this paper we discuss the properties of the Anderson model in the atomic ($V_k = 0$) limit

$$\mathcal{H}_a = \sum_{\sigma} E_{\sigma} n_{\sigma} + U n_{\uparrow} n_{\downarrow}, \quad (2)$$

for which only the last two terms in the Hamiltonian (1) remain.

3. SPIN AND CHARGE ALGEBRAS

Here we form the spin and charge operators \vec{S} and \vec{Q} . We also summarize some of their properties. We define the operator-valued spinor $\psi \equiv (d_\uparrow, d_\downarrow)^T$, and introduce spin-operator components as $S_\alpha \equiv \psi^\dagger \sigma_\alpha \psi$ for $\alpha \in \{x, y, z\}$ and $S^\pm \equiv (S_x \pm S_y) / \sqrt{2}$. Here σ_α are the usual Pauli spin matrices. Thus we obtain

$$S^+ = \frac{1}{\sqrt{2}} d_\uparrow^\dagger d_\downarrow \quad (3)$$

$$S^- = \frac{1}{\sqrt{2}} d_\downarrow^\dagger d_\uparrow \quad (4)$$

$$S_z = \frac{1}{2} (n_\uparrow - n_\downarrow) \quad (5)$$

$$S_z^2 = S_x^2 = S_y^2 = \frac{1}{4} (n_\uparrow + n_\downarrow - 2n_\uparrow n_\downarrow) = \frac{1}{3} S^2. \quad (6)$$

With the help of the spinor $\phi \equiv (d_\uparrow, d_\downarrow)^\dagger$, the charge-operator components may be expressed analogously in the form $Q_\alpha \equiv \phi^\dagger \sigma_\alpha \phi$. We find

$$Q^+ = \frac{1}{\sqrt{2}} d_\uparrow^\dagger d_\downarrow^\dagger \quad (7)$$

$$Q^- = \frac{1}{\sqrt{2}} d_\downarrow^\dagger d_\uparrow^\dagger \quad (8)$$

$$Q_z = \frac{1}{2} (n_\uparrow + n_\downarrow - 1) \quad (9)$$

$$Q_z^2 = Q_x^2 = Q_y^2 = \frac{1}{4} (1 - n_\uparrow - n_\downarrow + 2n_\uparrow n_\downarrow) = \frac{1}{3} Q^2. \quad (10)$$

From the operators \vec{S} and \vec{Q} , we can easily form a spin-1/2 algebra \vec{C} which obeys the canonical spin commutation relations $[C_i, C_j]_- = i\epsilon_{ijk} C_k$ with $C^2 = c(c+1)$ for $c = 1/2$, as follows. We note that \vec{S} and \vec{Q} obey by construction the canonical commutation relations. Moreover, for the atomic Anderson Hamiltonian we find that S_z and Q_z and thus S_z^2 and Q_z^2 (therefore, also S^2 and Q^2) are constants of motion. However, $\langle S^2 \rangle = \frac{3}{4}$ is not obeyed, unless $\langle Q^2 \rangle = 0$, and vice versa. Furthermore, one easily finds that $[S_i, Q_j] = 0$ for all i, j . Consequently, a spin-1/2 algebra \vec{C} can be formed as $\vec{C} \equiv \vec{S} + \vec{Q}$. One easily sees that $C^2 = S^2 + Q^2 = \frac{3}{4}$, as required for a spin of fixed magnitude 1/2. This clearly demonstrates the importance of considering both spin and charge degrees of freedom.

Response functions of an artificial Anderson atom in the atomic limit

4. EXPRESSIONS FOR THE SPIN AND CHARGE SUSCEPTIBILITIES

By utilizing the Hubbard operators³⁸

$$A_{1\sigma} \equiv (1 - n_{-\sigma}) d_{\sigma} \quad (11)$$

$$A_{2\sigma} \equiv n_{-\sigma} d_{\sigma} \quad (12)$$

(for a recent discussion of supersymmetric Hubbard operators, see³⁹) or the spin-flip and charge-transfer operators

$$A_{3\sigma} \equiv d_{-\sigma}^{\dagger} d_{\sigma} = \sqrt{2} S^{\pm} \quad (13)$$

$$A_{4\sigma} \equiv d_{-\sigma} d_{\sigma} = \sqrt{2} Q^{\pm} \quad (14)$$

the atomic Hamiltonian (2) may be represented as a bilinear form in two alternative pictures

$$\mathcal{H}_a = \Sigma_{\sigma} E_{\sigma} \left(A_{1\sigma}^{\dagger} A_{1\sigma} + A_{2\sigma}^{\dagger} A_{2\sigma} \right) + U A_{2\sigma}^{\dagger} A_{2\sigma} \quad (15)$$

$$= \Sigma_{\sigma} E_{\sigma} \left(A_{3\sigma}^{\dagger} A_{3\sigma} + A_{4\sigma}^{\dagger} A_{4\sigma} \right) + U A_{4\sigma}^{\dagger} A_{4\sigma}. \quad (16)$$

Action of the operators $A_{1\sigma}$, $A_{2\sigma}$, $A_{3\sigma}$ and $A_{4\sigma}$ and their hermitean adjoints on the states $|0\rangle$, $|\uparrow\rangle$, $|\downarrow\rangle$ and $|\uparrow\downarrow\rangle$ is shown in Table I. These operators are also eigenoperators of the Hamiltonian

$$[A_{k\sigma}, \mathcal{H}_a] = a_{k\sigma}(E, U, B) A_{k\sigma}, \quad (17)$$

where $a_{k\sigma}(E, U, B)$ is a scalar-valued function of the model parameters. Consequently, it is easy to obtain the following anticommutator (+) functions directly from the equations of motion (46) and (47) (no coupling to higher-order Green's functions)

$$\langle\langle A_{1\sigma}; A_{1\sigma}^{\dagger} \rangle\rangle_z^+ = \frac{\langle 1 - n_{-\sigma} \rangle}{z - E_{\sigma}} \quad (18)$$

$$\langle\langle A_{2\sigma}; A_{2\sigma}^{\dagger} \rangle\rangle_z^+ = \frac{\langle n_{-\sigma} \rangle}{z - E_{\sigma} - U} \quad (19)$$

$$\langle\langle A_{3\sigma}; A_{3\sigma}^{\dagger} \rangle\rangle_z^+ = \frac{\langle n_{\sigma} + n_{-\sigma} - 2n_{\sigma}n_{-\sigma} \rangle}{z + 2\sigma B} \quad (20)$$

$$\langle\langle A_{4\sigma}; A_{4\sigma}^{\dagger} \rangle\rangle_z^+ = \frac{\langle 1 - n_{\sigma} - n_{-\sigma} + 2n_{\sigma}n_{-\sigma} \rangle}{z - (2E + U)}. \quad (21)$$

The corresponding commutator (-) functions are found by replacing the expectation values in Eqs. (18)-(21), respectively, with $\langle (1 - n_{-\sigma})(1 - 2n_{\sigma}) \rangle$,

Table I

Operators $A_{1\sigma}$, $A_{2\sigma}$, $A_{3\sigma}$ and $A_{4\sigma}$ and their Hermitean adjoints describe all the possible transitions between the states $|0\rangle$, $|\uparrow\rangle$, $|\downarrow\rangle$ and $|\uparrow\downarrow\rangle$. Notation means that one obtains the final state $|f\rangle$ through the operation of an entry in the table on the initial state $|i\rangle$.

| final | initial | $ i\rangle$ | | | |
|-------------|------------------------------|---------------------------|---------------------------|-------------------------|------------------------------|
| | | $ 0\rangle$ | $ \uparrow\rangle$ | $ \downarrow\rangle$ | $ \uparrow\downarrow\rangle$ |
| | $ 0\rangle$ | $\hat{1}$ | $A_{1\uparrow}$ | $A_{1\downarrow}$ | $A_{4\uparrow}$ |
| $ f\rangle$ | $ \uparrow\rangle$ | $A_{1\uparrow}^\dagger$ | $\hat{1}$ | $A_{3\uparrow}^\dagger$ | $A_{2\downarrow}$ |
| | $ \downarrow\rangle$ | $A_{1\downarrow}^\dagger$ | $A_{3\uparrow}$ | $\hat{1}$ | $A_{2\uparrow}$ |
| | $ \uparrow\downarrow\rangle$ | $A_{4\uparrow}^\dagger$ | $A_{2\downarrow}^\dagger$ | $A_{2\uparrow}^\dagger$ | $\hat{1}$ |

$\langle n_{-\sigma} - 2n_\sigma n_{-\sigma} \rangle$, $\langle n_{-\sigma} - n_\sigma \rangle$ and $\langle 1 - n_\sigma - n_{-\sigma} \rangle$. Note that for the d electron we have $d_\sigma = A_{1\sigma} + A_{2\sigma}$ and for the d -electron propagator we find: $\langle\langle d_\sigma ; d_\sigma^\dagger \rangle\rangle_z^+ = \langle\langle A_{1\sigma} ; A_{1\sigma}^\dagger \rangle\rangle_z^+ + \langle\langle A_{2\sigma} ; A_{2\sigma}^\dagger \rangle\rangle_z^+ = \langle 1 - n_{-\sigma} \rangle / (z - E_\sigma) + \langle n_{-\sigma} \rangle / (z - E_\sigma - U)$, with poles at the single-particle eigenenergies of the atomic Hamiltonian (2), $z = E_\sigma$ and $z = E_\sigma + U$.

Considering the time correlation functions (50) and (51) for the Green's functions (18)–(21), one finds after some algebra

$$\langle n_\sigma \rangle = \frac{\langle n_\sigma n_{-\sigma} \rangle}{f(E_{-\sigma} + U)}, \quad (22)$$

where

$$\langle n_\sigma n_{-\sigma} \rangle = \frac{1 - f(E_\sigma) - f(E_{-\sigma})}{\frac{1}{f(2E + U)} - \frac{f(E_\sigma)}{f(E_\sigma + U)} - \frac{f(E_{-\sigma})}{f(E_{-\sigma} + U)}} \quad (23)$$

is the correlated double occupancy and f is the Fermi function.

Now we turn our attention to the longitudinal and transversal spin and charge response functions of the Anderson atom. They may be defined, for complex frequencies, as

$$\chi_\perp(z) \equiv -\langle\langle S^+ ; S^- \rangle\rangle_z^- = -\frac{1}{2} \langle\langle A_{3\downarrow} ; A_{3\downarrow}^\dagger \rangle\rangle_z^- \quad (24)$$

$$\xi_\perp(z) \equiv -\langle\langle Q^+ ; Q^- \rangle\rangle_z^- = -\frac{1}{2} \langle\langle A_{4\uparrow}^\dagger ; A_{4\uparrow} \rangle\rangle_z^- \quad (25)$$

$$\chi_\parallel(z) \equiv -\langle\langle (S_z - \langle S_z \rangle) ; (S_z - \langle S_z \rangle) \rangle\rangle_z^- \quad (26)$$

$$\xi_\parallel(z) \equiv -\langle\langle (Q_z - \langle Q_z \rangle) ; (Q_z - \langle Q_z \rangle) \rangle\rangle_z^- \quad (27)$$

Response functions of an artificial Anderson atom in the atomic limit

The expectation values $\langle S^\pm \rangle$ and $\langle Q^\pm \rangle$ vanish for \mathcal{H}_a and are thus not needed in the defining equations (24) and (25). However, $\langle S_z \rangle$ and $\langle Q_z \rangle$ in Eqs. (26) and (27) are generally nonzero. In connection with the $O(3)$ -symmetric Anderson model and the two-channel Kondo model, the charge operators are called isospin operators⁴⁰ and the parallel charge susceptibility is defined as a $Q_z - Q_z$ response as above but without extracting the mean.

The transversal spin susceptibility ($-$) function is readily found from Eq. (20) (changing the expectation value as described in the text after (20))

$$\chi_\perp(z) = -\frac{\langle S_z \rangle}{z - B}. \quad (28)$$

Consequently, the familiar static zero-frequency limit of $\chi_\perp(z)$ is found with (49)

$$\chi_\perp^0 = \int_{-\infty}^{\infty} \frac{d\omega}{\pi} \frac{\chi_\perp''(\omega)}{\omega} = \frac{\langle S_z \rangle}{B}. \quad (29)$$

Similarly, for the transversal charge susceptibility one obtains

$$\xi_\perp(z) = -\frac{\langle Q_z \rangle}{z + (2E + U)} \quad (30)$$

and

$$\xi_\perp^0 = \int_{-\infty}^{\infty} \frac{d\omega}{\pi} \frac{\xi_\perp''(\omega)}{\omega} = -\frac{\langle Q_z \rangle}{2E + U}. \quad (31)$$

Here $2E + U$ measures the asymmetry of the level configuration with respect to the Fermi level, vanishing in the symmetric ($E = -U/2$) situation. Thus asymmetry behaves for the charge degrees of freedom as the magnetic field for the spin degrees of freedom (compare Eqs. (29) and (31)).

For the parallel spin response in Eq. (26), one cannot directly calculate the commutator ($-$) function with the equations of motion (46) and (47) since $[S_z - \langle S_z \rangle, S_z - \langle S_z \rangle] = 0$, and also $[S_z - \langle S_z \rangle, \mathcal{H}_a] = 0$. However the corresponding anticommutator function is easy to find since $\{S_z - \langle S_z \rangle, S_z - \langle S_z \rangle\} = 2(\langle S_z^2 \rangle - \langle S_z \rangle^2)$, after which the static parallel spin susceptibility χ_\parallel^0 is obtained with the help of the fluctuation-dissipation theorem (54). The result is

$$\chi_\parallel^0 = \frac{\langle S_z^2 \rangle - \langle S_z \rangle^2}{T}. \quad (32)$$

For the parallel charge response, a similar calculation yields

$$\xi_\parallel^0 = \frac{\langle Q_z^2 \rangle - \langle Q_z \rangle^2}{T}. \quad (33)$$

The parallel susceptibilities may, furthermore, be calculated from

$$\chi_\parallel^0 = \frac{\partial \langle S_z \rangle}{\partial B}, \quad (34)$$

Ari T. Alastalo, Markku P. V. Stenberg, and Martti M. Salomaa

and

$$\xi_{\parallel}^0 = - \left. \frac{\partial \langle Q_z \rangle}{\partial (2E + U)} \right|_U, \quad (35)$$

where the partial derivation is performed such that the intra-atomic Coulomb repulsion U is held constant.

The expectation values $\langle S_z \rangle$, $\langle S_z^2 \rangle$, $\langle Q_z \rangle$ and $\langle Q_z^2 \rangle$ in the above results for the response functions are expressible through $\langle n_{\sigma} \rangle$ and $\langle n_{\sigma} n_{-\sigma} \rangle$ as shown in Section 3. Furthermore, since we know $\langle n_{\sigma} \rangle$ and $\langle n_{\sigma} n_{-\sigma} \rangle$ from Eqs. (22) and (23), respectively, it is now straightforward to find the susceptibilities. In terms of the dimensionless parameters

$$\begin{aligned} x &\equiv T/U, & y &\equiv E/U, & b &\equiv B/T, \\ \mathcal{E} &\equiv e^{y/x} + e^{b/2} + e^{-b/2} + e^{(-1-y)/x} \end{aligned} \quad (36)$$

the final results are

$$T\chi_{\perp}^0 = \sinh\left(\frac{b}{2}\right) / (b\mathcal{E}) \quad (37)$$

$$T\chi_{\parallel}^0 = \left\{ 1 + \frac{1}{2} \cosh\left(\frac{b}{2}\right) [e^{y/x} + e^{(-1-y)/x}] \right\} / \mathcal{E}^2 \quad (38)$$

$$T\xi_{\perp}^0 = x [e^{y/x} - e^{(-1-y)/x}] / [2(1+2y)\mathcal{E}] \quad (39)$$

$$T\xi_{\parallel}^0 = \left\{ e^{-1/x} + \frac{1}{2} \cosh\left(\frac{b}{2}\right) [e^{y/x} + e^{(-1-y)/x}] \right\} / \mathcal{E}^2. \quad (40)$$

In what follows, we omit the superscript zero from $\chi_{\perp, \parallel}^0$ and $\xi_{\perp, \parallel}^0$ since in this paper we only consider the static response functions.

In addition, we mention the following properties obeyed in the zero-field and symmetric limits for the static responses

$$\lim_{B \rightarrow 0} \chi_{\parallel} = \lim_{B \rightarrow 0} \chi_{\perp} \quad (41)$$

$$\lim_{E \rightarrow -U/2} \xi_{\parallel} = \lim_{E \rightarrow -U/2} \xi_{\perp}. \quad (42)$$

The equalities (41) and (42) again demonstrate that the asymmetry is analogous to an external magnetic field when one considers the charge response functions instead of the spin susceptibilities. All the response functions are symmetric with respect to reversal of the external field ($B \rightarrow -B$). What is more interesting, however, is that the susceptibilities are also symmetric with respect to reversal of asymmetry ($a \equiv 2E + U \rightarrow -a$).

Response functions of an artificial Anderson atom in the atomic limit

5. RESULTS

Here we consider the magnetic-field and level-asymmetry dependencies of the spin and charge response functions, $\chi_{\parallel,\perp}(T)$ and $\xi_{\parallel,\perp}(T)$. We keep U constant and vary E (or y), such that there is a one-to-one relationship between $y \equiv E/U$ and asymmetry $a \equiv 2E + U = U(2y + 1)$. Consequently, the curves are seen to be drawn for varying level asymmetries. Figures 1–7 are for $U > 0$ while Figs. 8–12 describe the negative- U situation. The dashed curves always denote $y < 0$, while the solid ones are for $y \geq 0$. Furthermore, we have labelled the curves such that the field parameter $b \equiv B/T$ is shown inside the parentheses. When the field parameter is omitted, $b = 0$ is implied. Owing to the above-mentioned symmetry of the response functions with respect to reversal of asymmetry, it is convenient to consider positive asymmetries only for $U > 0$ and negative asymmetries for $U < 0$. In particular, this means that $y \geq -1/2$ below.

The number of illustrations that follow is large. However, we explore the four response functions to illustrate their interrelationships and symmetries upon reversal of U with varying level asymmetries and external field strengths.

5.1. Positive U

5.1.1. Zero External Field

Figure 1 shows the spin susceptibility in zero external field ($\chi_{\perp} = \chi_{\parallel}$) for various asymmetries. This is also given in reference.⁹ We observe that the Curie law for a quantum-mechanical spin one half, $T\chi = 1/4$, is best obeyed in the low-temperature limit for the symmetric situation (curve "a"). However, for $y < 0$, the spin susceptibility always finally rises to the level $(4T)^{-1}$ for low enough temperatures. This happens simultaneously with the depression of the parallel charge susceptibility, see Fig. 2. Also the perpendicular charge susceptibility vanishes at low temperatures for all configurations, see Fig. 7a. It is thus legitimate to state that the spin degrees of freedom are the relevant low-energy (or strong- U) excitations for $U > 0$. Furthermore, we find for zero field ($\langle S_z \rangle = 0$)

$$T\chi + T\xi_{\parallel} + \langle Q_z \rangle^2 = T\chi + T\xi_{\parallel} + \left(\frac{2y + 1}{T/U}\right)^2 (T\xi_{\perp})^2 = \frac{1}{4}. \quad (43)$$

Therefore, as the charge susceptibilities vanish for low temperatures, we obtain $T\chi = 1/4$, as already stated. For high temperatures ($T \gg U$), on the other hand, the oscillator strength becomes evenly distributed among the spin and charge degrees of freedom and the spin and charge susceptibilities

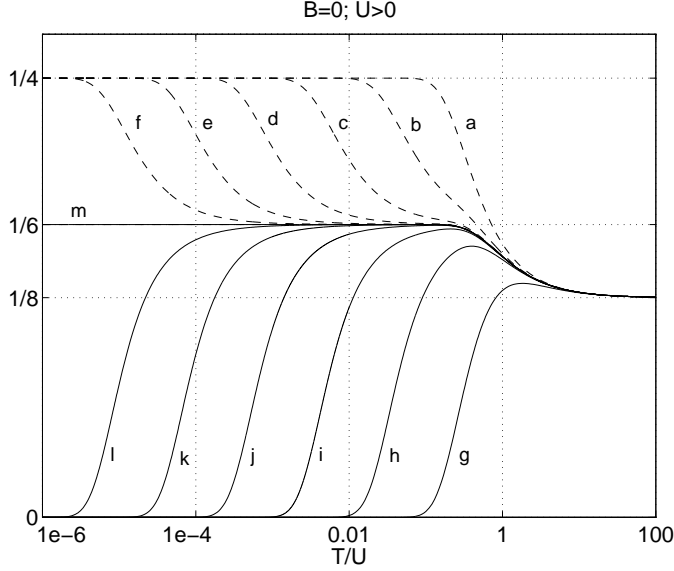


Fig. 1. Curie parameter $T\chi$ in zero external field ($\chi_{\parallel} \equiv \chi_{\perp}$) for positive U as a function of level asymmetry. Here $|y| \in \{0\} \cup \{\frac{1}{2^p} \mid p \in \{1, 4, 7, 10, 13, 16\}\}$, such that for the curves "a" \rightarrow "f" ("g" \rightarrow "l"), y is negative (positive). The curve labeled "m" denotes $y = 0$.

approach the common value $\lim_{T/U \rightarrow \infty} T\chi = \lim_{T/U \rightarrow \infty} T\xi = 1/8$ in zero field for all values of y , *c.f.* Figs. 1, 2 and 7a.

The $y = 0$ configuration is a special case. From the general result for the spin-state occupations in Eq. (22), it is easy to see that here the occupation numbers satisfy: $\langle n_{\uparrow} \rangle = \langle n_{\downarrow} \rangle = 1/3$, which yields $\langle Q_z \rangle^2 = 1/36$, see Eq. (10). Consequently, one finds that the low-temperature limits in zero field for $y = 0$: $T\chi = 1/6$, $T\xi_{\parallel} = 1/18$ and $T\xi_{\perp} \rightarrow 0$ are consistent with the result in Eq. (43).

5.1.2. Finite Field

Figures 3a and 4a show the field dependencies of the longitudinal and perpendicular spin susceptibilities, respectively, for weak fields. One observes that the longitudinal component is more strongly affected by the external magnetic field. Furthermore, in high fields – Figs. 3b and 4b – the longitudinal spin response displays peaks of invariant height for $y > 0$, whereas the transversal function exhibits threshold behaviour. These peaks and thresholds correspond to the situation where one of the localized energy

Response functions of an artificial Anderson atom in the atomic limit

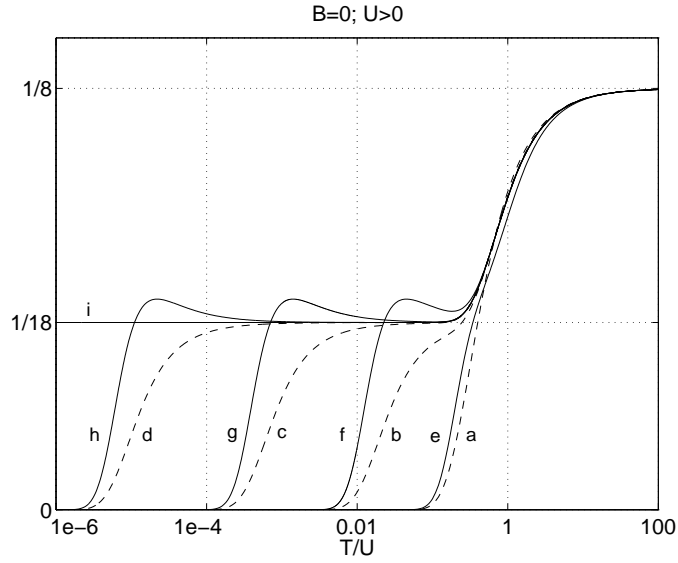


Fig. 2. Curie parameter for the charge susceptibility $T\xi_{\parallel}$ with $U > 0$ for vanishing magnetic field as a function of asymmetry. Here $|y| \in \{0\} \cup \{\frac{1}{2^p} \mid p \in \{1, 5, 10, 16\}\}$, such that for the curves "a" \rightarrow "d" ("e" \rightarrow "h"), y is negative (positive). The curve labeled "i" denotes $y = 0$.

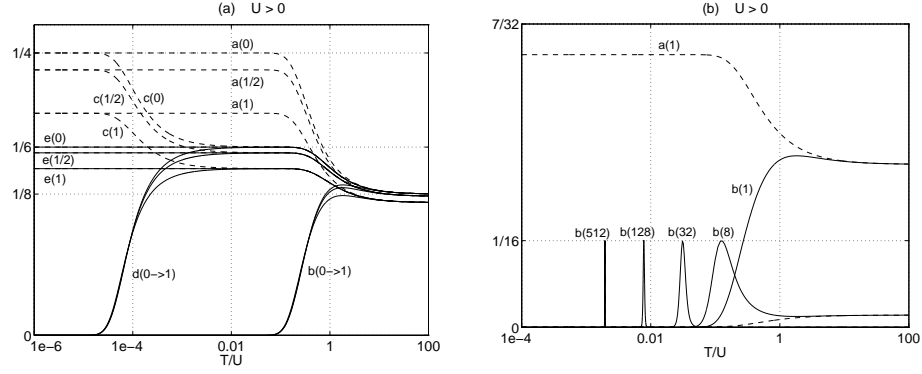


Fig. 3. Magnetic-field dependence of the longitudinal magnetic susceptibility $\chi_{\parallel}(B, T)$ in (a) moderate and (b) extreme fields. The curves "a" and "b" are for $|y| = 1/2$ while "c" and "d" denote $|y| = 1/(2^{13})$. The curves for which $y = 0$ are labeled "e". Magnetic field is measured in terms of $b = B/T$ which is indicated in the parentheses in this figure.

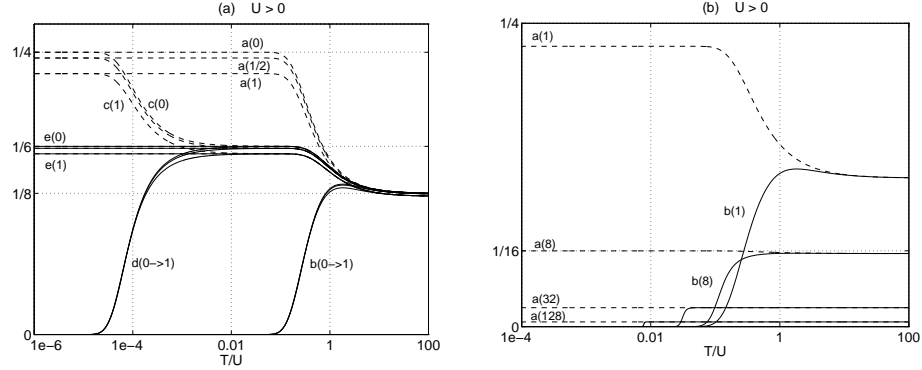


Fig. 4. Magnetic field dependence of the transversal spin susceptibility $\chi_{\perp}(B, T)$ in (a) moderate and (b) extreme fields.

levels crosses the Fermi level as shown in Fig. 5a for $y = 1/2$. The height of the peaks in $T\chi_{\parallel}$ is $1/16$, irrespective of the absolute value of y .

The parallel and perpendicular charge response functions for weak and strong fields are considered in Figs. 6 and 7. Also for the charge susceptibility, the parallel component is peaked at high fields for $y > 0$ at the level $1/16$. This is shown in Fig. 6b for $y = 1/2$ in which case the peak again occurs in the level configuration of Fig. 5a. Simultaneously, the perpendicular charge susceptibility shows threshold dependence, see Fig. 7b. In Fig. 7a, for $T\xi_{\perp}$ the curve for $y = 0$ would lie between the $|y| = 1/16$ curves shown in the figure.

Response functions of an artificial Anderson atom in the atomic limit

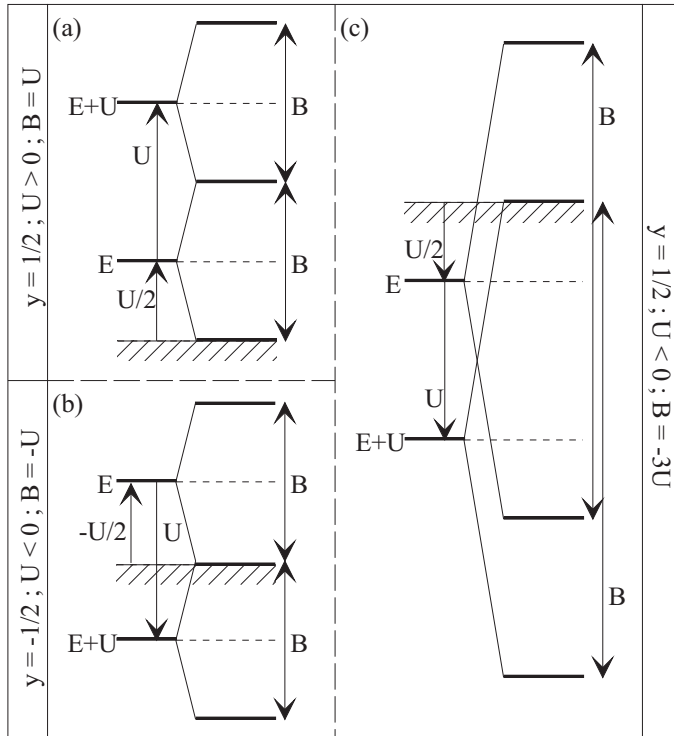


Fig. 5. Special values of large applied magnetic fields yield level configurations with particular symmetry. These level schemes correspond to distinct features in the magnetic and charge response functions (a: c.f., Figs. 3b, 4b, 6b, 7b; b: c.f., Figs. 11b, 12b; c: c.f., Figs. 9b, 10b, 11b, 12b).

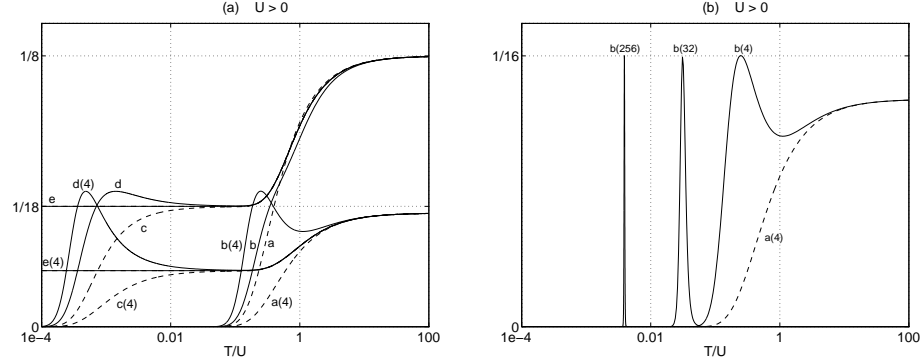


Fig. 6. Field dependence of the parallel charge susceptibility ξ_{\parallel} in (a) moderate and (b) extreme fields. The curves "a" and "b" are for $|y| = 1/2$ while "c" and "d" denote $|y| = 1/(2^{10})$. The curves for which $y = 0$ are labeled "e". The zero-field situation was already considered in Fig. 2.

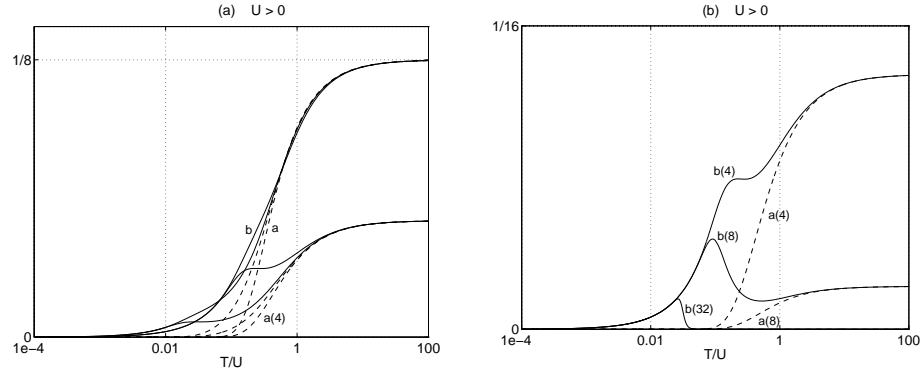


Fig. 7. Field- and asymmetry dependence of the perpendicular charge susceptibility ξ_{\perp} for $U > 0$ in (a) moderate and (b) extreme fields. The curves "a" and "b" are for $|y| = 1/2$ while "c" and "d" denote $|y| = 1/16$.

Response functions of an artificial Anderson atom in the atomic limit

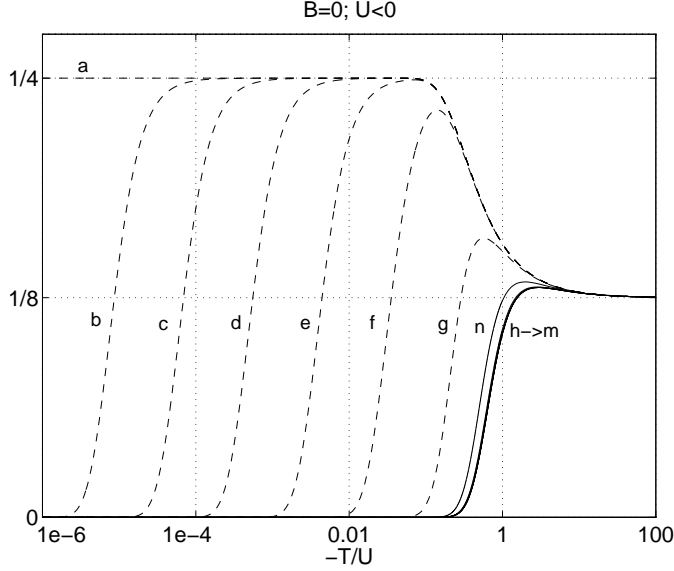


Fig. 8. Asymmetry dependence of the longitudinal zero-field charge susceptibility, $\xi_{\parallel}(B = 0, T)$, for $U < 0$. Here $|y| \in \{\frac{1}{2}\} \cup \{\frac{2^p-1}{2^{p+1}} \mid p \in \{16, 13, 10, 7, 4, 1\}\}$, such that for the curves "a" \rightarrow "g" ("h" \rightarrow "n"), y is negative (positive).

5.2. Negative U

The charge susceptibility in zero field and for weak and strong magnetic fields is illustrated in Figs. 8 and 9 for the parallel component and in Fig. 10 for the perpendicular part. The low-temperature charge Curie law $T\xi = 1/4$ is here found to be obeyed only in the symmetric situation ($y = -1/2$, $\xi_{\perp} = \xi_{\parallel}$), irrespective of the magnetic field. Furthermore, an infinitesimal asymmetry is sufficient to depress the low-temperature limit as shown in Fig. 8a, where the curve "b" corresponds to $y \approx -0.499992$. Again, in high fields a peak of height $1/16$ is formed in the parallel charge response $T\xi_{\parallel}$ for $y > 0$, while the perpendicular component displays a threshold at the same point. However, here for $y = 1/2$ this behaviour corresponds to the level configuration shown in Fig. 5c, where $B = -3U$.

For $U < 0$ the spin susceptibilities behave in a similar way as the charge response functions for $U > 0$, freezing out for low enough temperatures, as shown in Figs. 11 and 12. However, the $y = 0$ situation is not a special case here. Again we observe that the parallel spin susceptibility is more sensitive

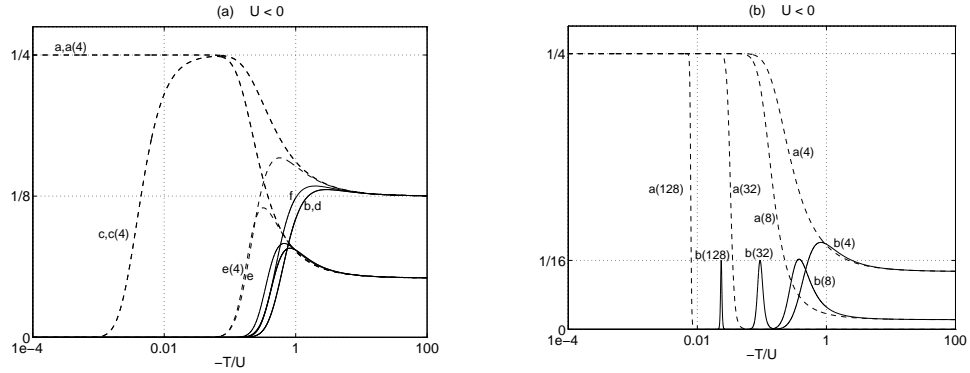


Fig. 9. Field dependence of ξ_{\parallel} , for $U < 0$ in (a) moderate and (b) extreme fields. The curves "a" and "b" are for $|y| = 1/2$, "c" and "d" denote $|y| = 127/256$ and the curves for which $|y| = 1/4$ are labeled "e" and "f".

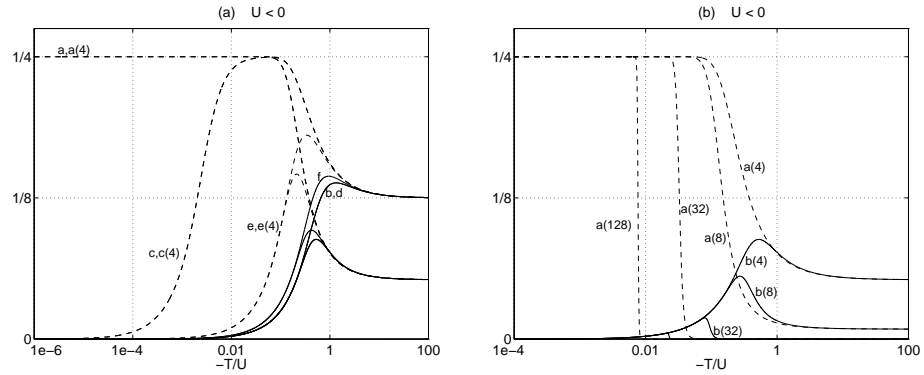


Fig. 10. Field dependence of ξ_{\perp} , for $U < 0$ in (a) moderate and (b) strong fields.

Response functions of an artificial Anderson atom in the atomic limit

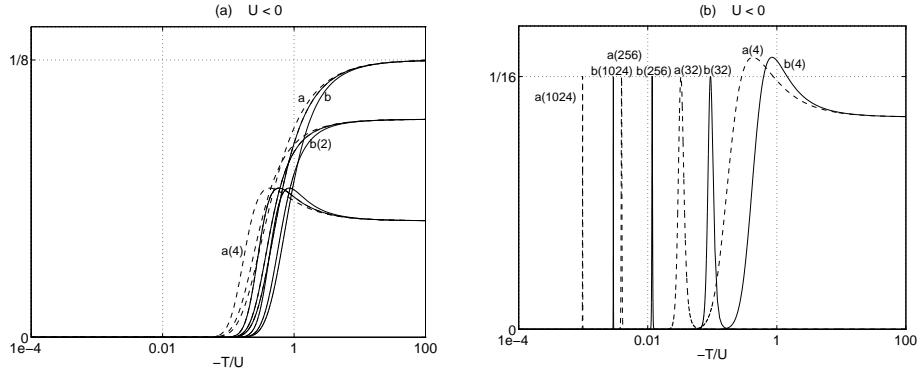


Fig. 11. (a) For $U < 0$, the longitudinal spin susceptibility χ_{\parallel} is strongly suppressed for $T < U/10$. (b) A sharp peak is formed for extreme fields for both positive and negative values of y . Curves "a" and "b" are for $|y| = 1/2$, corresponding to level configurations in Figs. 5b and 5c, while the other curves in (a) represent $|y| = 1/2^{10}$.

to the external field than the perpendicular component. Furthermore, we find peaks in $T\chi_{\parallel}$ and thresholds in $T\chi_{\perp}$ for high fields, but now both at $y > 0$ and $y < 0$. The $y = 1/2$ peaks and thresholds in Figs. 11b and 12b correspond to the level configuration of Fig. 5c ($B = -3U$), while those for $y = -1/2$ correspond to the situation in Fig. 5b, where $B = -U$.

5.3. Contrasting Spin and Charge

As pointed out above, the reversal of U exchanges the mutual roles of the spin and charge degrees of freedom. We find, in particular, that at zero field for the symmetric situation ($y = -1/2$): $\xi(U < 0) = \chi(U > 0)$ and $\xi(U > 0) = \chi(U < 0)$. This is illustrated in Fig. 13 for the parallel susceptibilities. Furthermore, we find that the spin and charge response functions are symmetric with respect to the level asymmetry $a = 2E + U$, such that $\chi(a) = \chi(-a)$ and $\xi(a) = \xi(-a)$ are obeyed.

6. DISCUSSION

The Anderson impurity model has proven capable of describing a remarkable variety of different physical systems in the field of strongly correlated electrons. Presently, an important trend in condensed-matter physics and nanoelectronics is one where artificial man-made objects are studied, rather than real atoms or molecules. The progress in lithography techniques has made it possible, e.g., to fabricate quantum dots with properties similar to those of real atoms. Our study has relevance for such systems where

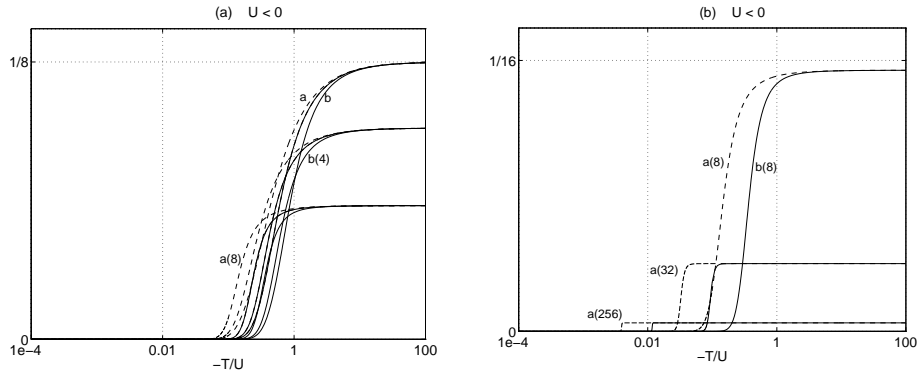


Fig. 12. (a) For $U < 0$, the transversal spin susceptibility χ_{\perp} is strongly suppressed at low temperatures. (b) Extreme field values produce a threshold for both $y > 0$ and $y < 0$ corresponding to the peaks in Fig. 11. The curves have been drawn for the same asymmetries as in Fig. 11.

isolated localized energy levels occur. It would be interesting to investigate whether indications for negative- U behaviour previously found, e.g., in the context of high-temperature superconductivity and heavy-fermion systems could also be experimentally realized in quantum dots⁴¹ or carbon nanotubes with magnetic impurities.

We have studied the spin and charge susceptibilities of an artificial Anderson atom for arbitrary values of the model parameters. General results for all the four relevant response functions have here been presented to the best of our knowledge for the first time and an extensive survey of the properties of these susceptibilities was carried out. It was pointed out, in particular, how the level asymmetry behaves for the charge degrees of freedom as the magnetic field for the spin, and that the reversal of U changes the mutual roles of spin and charge. In particular, for low temperatures and with positive U , the Curie law for a free spin-1/2 is followed by the spin response, whereas the charge excitations become suppressed. On the other hand, for negative U at low temperatures, the charge susceptibility follows the Curie law in the symmetric case, whereas the spin responses vanish. At high temperatures and for increasing asymmetry, the transfer of oscillator strength from the spin degrees of freedom to the charge modes becomes increasingly important. In the $T \rightarrow \infty$ limit, thermal fluctuations average over any details in the energy-level structure. Consequently, the spin and charge modes have equal oscillator strengths and they become equally relevant.

It is noted that for increasing magnetic-field strength, the longitudinal susceptibilities are more strongly suppressed than the perpendicular components. Furthermore, at extremely high fields, the longitudinal responses show peaks of invariant height while the perpendicular responses have a

Response functions of an artificial Anderson atom in the atomic limit

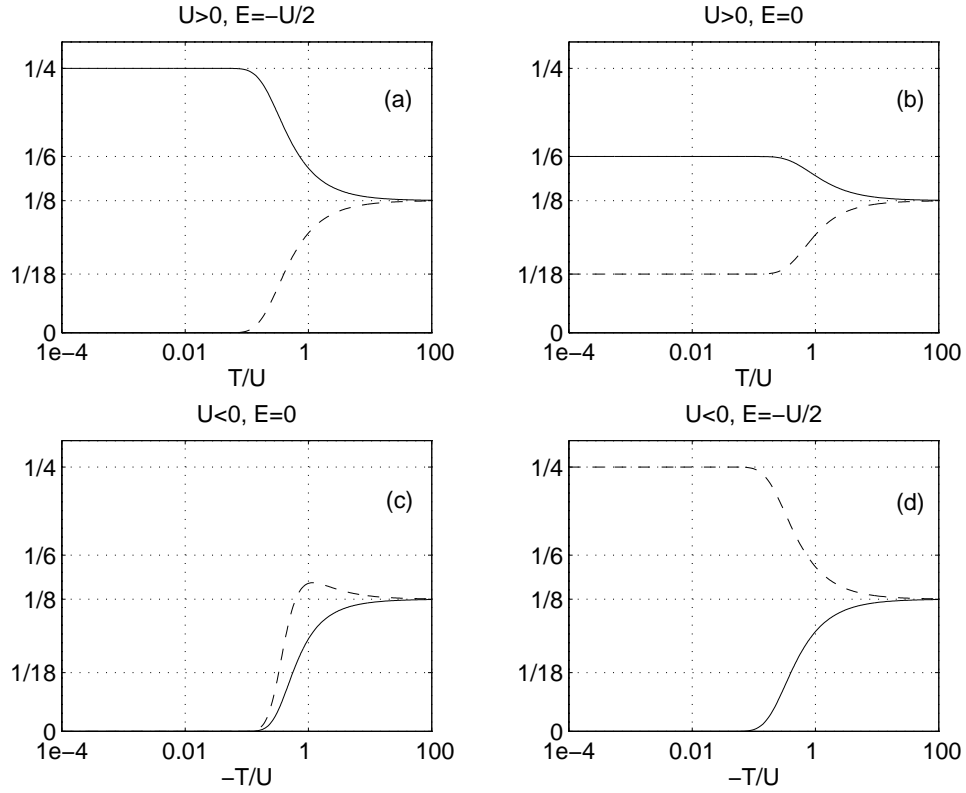


Fig. 13. Contrasting spin (χ_{\parallel}) (solid line) and charge (ξ_{\parallel}) (dashed line) response functions for $U > 0$ (a and b) and for $U < 0$ (c and d). Note, in particular, the spin-charge duality: exchange in the roles of χ and ξ for $U \leftrightarrow -U$ (between a and d). For further discussion, see the main body of text.

Ari T. Alastalo, Markku P. V. Stenberg, and Martti M. Salomaa

threshold. These features are associated with particular level crossings, as discussed in the text.

Our thorough discussion of the spin and charge (pseudospin) susceptibilities in the atomic limit of the Anderson model has revealed several new and interesting details in these response functions. These new features are expected to be particularly relevant in connection with the behaviour of quantum dots since in this case it is possible to create very high effective magnetic fields far beyond those encountered in atomic physics. Therefore, quantum dots serve as interesting laboratory models for Anderson model physics in limits which have not been explored before. Our results serve to emphasize and increase understanding of the relationships governing the spin-charge duality in the atomic limit of the Anderson model. The atomic model can be taken as the starting point of perturbation expansions in the Schrieffer-Wolff limit where the Anderson model can be related to the Kondo model for magnetic impurities in metals.⁴³ Unified definitions of spin and charge susceptibilities have been given and they will be utilized in future works.

A. RESPONSE FUNCTIONS

In order to describe the response of an operator A due to a perturbation coupled to operator B , it is natural to investigate the generalized admittance function,⁷ defined in Zubarev's⁴² notation as

$$\langle\langle A; B \rangle\rangle_z^{(\pm)} = \mp i \int_{-\infty}^{\infty} dt e^{izt} \theta(\pm t) \langle\langle [A(t), B(0)]_{(\pm)} \rangle\rangle, \quad (44)$$

which is a complex function of the frequency variable z and has been analytically continued for complex arguments. The upper and lower signs designate $\text{Im}(z) > 0$ and $\text{Im}(z) < 0$, respectively, and correspond to the retarded (analytic in the upper half of the complex plane) and advanced (analytic in the lower halfplane) functions. The superscript (+) refers to an anticommutator ($[A, B]_{(+)} \equiv \{A, B\}$, correlation) function, while a commutator ($[A, B]_{(-)} \equiv [A, B]$, response) function is meant with the superscript (-). Do not confuse (\pm) (signs in parentheses) marking the commutator (-) and anticommutator (+) functions with \pm or \mp (without parentheses) denoting the retarded and advanced functions in (44).

The time evolution of operators is ruled in the Heisenberg representation by the operator equation

$$A(t) = e^{i\mathcal{H}t} A(0) e^{-i\mathcal{H}t}, \quad (45)$$

where \mathcal{H} is the Hamiltonian. Partial integration of (44) yields with the help

Response functions of an artificial Anderson atom in the atomic limit

of (45) the equations of motion

$$z\langle\langle A; B \rangle\rangle_z^{(\pm)} = \langle[A, B]_{(\pm)}\rangle + \langle\langle[A, \mathcal{H}]; B \rangle\rangle_z^{(\pm)} \quad (46)$$

$$= \langle[A, B]_{(\pm)}\rangle - \langle\langle A; [B, \mathcal{H}] \rangle\rangle_z^{(\pm)}, \quad (47)$$

where the ensemble averages $\langle \rangle$ can be related selfconsistently to the respective admittance functions (see below). For most of the nontrivial Hamiltonians of interest, the equations of motion for the relevant double-time Greens functions constitute an infinite hierarchy, whose termination (*e.g.*, in the Hartree-Fock approximation) has been a frequently employed approximation technique in the theory of magnetism. It is therefore of interest to consider models where the exact double-time functions can in fact be evaluated in closed form.

For large frequencies, the double-time functions decrease at least as $\langle\langle A; B \rangle\rangle \sim z^{-1}$, as can be readily seen from their equations of motion (46) and (47). Moreover, these functions are analytic off the real frequency (ω) axis, across which there exists a cut discontinuity

$$\langle\langle A; B \rangle\rangle_{\omega \pm i0} = \langle\langle A; B \rangle\rangle_{\omega}' \pm i\langle\langle A; B \rangle\rangle_{\omega}'' \quad (48)$$

where the prime superscript denotes the real part, while the double prime stands for the imaginary part of the function. Thus the response functions may be represented using the Hilbert transformation

$$\langle\langle A; B \rangle\rangle_z = \int \frac{d\omega}{\pi} \frac{\langle\langle A; B \rangle\rangle_{\omega}''}{\omega - z}, \quad (49)$$

which is also called spectral representation.

For the anticommutator (+) metric, the time-correlation functions (expectation values) may be obtained using

$$\langle\delta A(t) \delta B(0)\rangle = \int \frac{d\omega}{\pi} e^{-i\omega t} [1 - f(\omega)] G_{AB}''(\omega) \quad (50)$$

$$\langle\delta B(0) \delta A(t)\rangle = \int \frac{d\omega}{\pi} e^{-i\omega t} f(\omega) G_{AB}''(\omega), \quad (51)$$

where $\delta A = A - \langle A \rangle$, $\delta B = B - \langle B \rangle$, $G_{AB}(z) = -\langle\langle A; B \rangle\rangle_z^+$ and $f(\omega)$ is the Fermi distribution function (temperature units are chosen such that the Boltzmann constant is unity). For the commutator (response, (-)) functions we have

$$\langle\delta A(t) \delta B(0)\rangle = \int \frac{d\omega}{\pi} e^{-i\omega t} [1 + n(\omega)] \chi_{AB}''(\omega) \quad (52)$$

$$\langle\delta B(0) \delta A(t)\rangle = \int \frac{d\omega}{\pi} e^{-i\omega t} n(\omega) \chi_{AB}''(\omega), \quad (53)$$

Ari T. Alastalo, Markku P. V. Stenberg, and Martti M. Salomaa

where the $A - B$ susceptibility is defined as $\chi_{AB}(z) = -\langle\langle A; B \rangle\rangle_z^-$ and $n(\omega)$ is the Bose function. Furthermore, the fluctuation-dissipation theorem

$$G''_{AB}(\omega) = \coth\left(\frac{\omega}{2T}\right) \chi''_{AB}(\omega) \quad (54)$$

gives a relation between the commutator and anticommutator functions.

ACKNOWLEDGMENTS

Part of this work was carried out at the Institute für Theorie der Kondensierten Materie at the Universität Karlsruhe, Germany. MMS is grateful to P. Wölfle for cordial hospitality, G. Schön for discussions and the HER-AEUS Foundation for financial support. MPVS acknowledges the support by the Finnish Cultural Foundation. This work has also been supported by the Academy of Finland through the project "Theoretical Materials Physics".

REFERENCES

1. R. C. Ashoori, *Nature* **379**, 413 (1996).
2. S. M. Cronenwett, T. H. Oosterkamp, and L. P. Kouwenhoven, *Science* **281**, 540 (1998).
3. N. H. Bondaeo, J. Erland, D. Gammon, D. Park, D. S. Katzer, D. G. Steel, *Science* **282**, 1473 (1998).
4. Y. Meir, N. S. Wingreen, and P. A. Lee, *Phys. Rev. Lett.* **66**, 3048 (1991).
5. Y. Alhassid, *Rev. Mod. Phys.* **72**, 895 (2000).
6. P. W. Anderson, *Phys. Rev.* **124**, 41 (1961).
7. G. Rickayzen, *Green's Functions and Condensed Matter* (Academic Press, 1981); S. Doniach and E. H. Sondheimer, *Green's Functions for Solid State Physicists* (Imperial College Press, 1974); E. N. Economou, *Green's Functions in Quantum Physics* (Springer, 1983).
8. W. Weller, *Phys. Status Solidi (b)* **162**, 251 (1990).
9. H. R. Krishna-murthy, J. W. Wilkins, and K. G. Wilson, *Phys. Rev. B* **21**, 1003 (1980); **21**, 1044 (1980).
10. R. Bulla, A. C. Hewson, and Th. Pruschke, *J. Phys.: Condens. Matter* **10**, 8365 (1998).
11. P. B. Wiegmann and A. M. Tselick, *J. Phys. C: Solid State Phys.* **16**, 2281 (1983); **16**, 2321 (1983).
12. P. S. Riseborough, *Phys. Rev. B* **67**, 045102 (2003).
13. K. Yosida and K. Yamada, *Prog. Theor. Phys. Suppl.* **46**, 244 (1970).
14. K. Yamada, *Prog. Theor. Phys.* **53**, 970 (1975).
15. M. M. Salomaa, *Solid State Commun.* **38**, 815 (1981); **39**, 1105 (1981).
16. F. Wei, J.-L. Zhu, and H.-M. Chen, *Phys. Rev. B* **67**, 125410 (2003).
17. J. Brinckmann, *Phys. Rev. B* **54**, 10465 (1996).
18. M. E. Foglio and M. S. Figueira, *Phys. Rev. B* **60**, 11361 (1999).
19. G. Czycholl, A. L. Kuzemsky, and S. Wernbter, *Europhys. Lett.* **34**, 133 (1996).

Response functions of an artificial Anderson atom in the atomic limit

20. D. Meyer, T. Wegner, M. Potthoff, and W. Nolting, *Physica B: Condensed Matter* **270**, 225 (1999).
21. O. Takagi and T. Saso, *J. Phys. Soc. Japan* **68**, 2894 (1999).
22. A. C. Hewson, *The Kondo Problem to Heavy Fermions* (Cambridge University Press, 1993).
23. P. W. Anderson, *Phys. Rev.* **112**, 1900 (1958).
24. The superscript zero denotes static response.
25. P. W. Anderson, *Phys. Rev. Lett.* **34**, 953 (1975).
26. S. R. Micnas, J. Ranninger, and S. Robaszkiewicz, *Rev. Mod. Phys.* **62**, 113 (1990).
27. A. Taraphder and P. Coleman, *Phys. Rev. Lett.* **66**, 2814 (1991).
28. R. D. Harris, J. L. Newton, and G. D. Watkins, *Phys. Rev. B* **36**, 1094 (1987).
29. S. Ghosh and V. Kumar, *Phys. Rev. B* **46**, 7533 (1992).
30. R. C. Ashoori, H. L. Stormer, J. S. Weiner, L. N. Pfeiffer, S. J. Pearton, K. W. Baldwin and K. W. West, *Phys. Rev. Lett.* **68**, 3088 (1992).
31. R. C. Ashoori, H. L. Stormer, J. S. Weiner, L. N. Pfeiffer, S. J. Pearton, K. W. Baldwin, and K. W. West, *Physica (Amsterdam)* **189B**, 117 (1993).
32. N. B. Zhitenev, R. C. Ashoori, L. N. Pfeiffer, and K. W. West, *Phys. Rev. Lett.* **79**, 2308 (1997).
33. R. C. Ashoori, N. B. Zhitenev, L. N. Pfeiffer, and K. W. West, *Physica (Amsterdam)* **3E**, 15 (1998).
34. M. Brodsky, N. B. Zhitenev, R. C. Ashoori, L. N. Pfeiffer, and K. W. West, *Phys. Rev. Lett.* **85**, 2356 (2000).
35. Y. Wan, G. Ortiz, and P. Phillips, *Phys. Rev. Lett.* **75**, 2879 (1995).
36. M. E. Raikh, L. I. Glazman, and L. E. Zhukov, *Phys. Rev. Lett.* **77**, 1354 (1996).
37. M. M. Salomaa, *Z. Phys. B* **25**, 49 (1976).
38. J. Hubbard, *Proc. R. Soc. A* **281**, 401 (1964).
39. J. Hopkinson and P. Coleman, *Phys. Rev. B* **67**, 085110 (2003).
40. S. C. Bradley, R. Bulla, A. C. Hewson, and G. M. Zhang, *Eur. Phys. J. B* **11**, 535 (1999).
41. P. Schlottmann and A. A. Zvyagin, *Phys. Rev. B* **67**, 115113 (2003).
42. D. N. Zubarev, *Sov. Phys. Usp.* **3**, 320 (1960).
43. J. R. Schrieffer and P. A. Wolff, *Phys. Rev.* **149**, 491 (1966).